Journal of Catalysis **189,** 253–262 (2000)
doi:10.1006/jcat.1999.2513, available online at http://www.idealibrary.com on IDEAL®

A Study of the Kinetics and Mechanism of the Adsorption and Anaerobic Partial Oxidation of *n*-Butane over a Vanadyl Pyrophosphate Catalyst

B. H. Sakakini,* Y. H. Taufiq-Yap,† and K. C. Waugh*

*Department of Chemistry, UMIST, P.O. Box 88, Manchester M60 1QD, United Kingdom; and
†Department of Chemistry, Universiti Putra Malaysia, 43400 UPM Serdang, Malaysia

Received September 23, 1998; revised February 3, 1999; accepted March 29, 1999

The interaction of *n*-butane with a ($(VO)_2P_2O_7$) catalyst has been investigated by temperature-programmed desorption and anaerobic temperature-programmed reaction. *n*-Butane has been shown to adsorb on the $(VO)_2P_2O_7$ to as a butyl–hydroxyl pair. When adsorption is carried out at 223 K, upon temperature programming some of the butyl–hydroxyl species recombine resulting in butane desorption at 260 K. However, when adsorption is carried out at 423 K, the hydroxyl species of the butyl–hydroxyl pair migrate away from the butyl species during the adsorption, forming water which is detected in the gas phase. Butane therefore is not observed to desorb at 260 K after we lowered the temperature to 223 K under the butane/helium from the adsorption temperature of 423 K prior to temperature programming from that temperature to 1100 K under a helium stream. Anaerobic temperature-programmed oxidation of *n*-butane produces butene and butadiene at a peak maximum temperature of 1000 K; this is exactly the temperature at which, upon temperature programming, oxygen evolves from the lattice and desorbs as O_2. This, and the fact that the amount of oxygen desorbing from the $(VO)_2P_2O_7$ at ~1000 K is the same as that required for the oxidation of the *n*-butane to butene and butadiene, strongly suggests (i) that lattice oxygen as it emerges at the surface is the selective oxidant and (ii) that its appearance at the surface is the rate-determining step in the selective oxidation of *n*-butane. The surface of the $(VO)_2P_2O_7$ catalyst on which this selective oxidation takes place has had approximately two monolayers of oxygen removed from it by unselective oxidation of the *n*-butane to CO, CO_2, and H_2O between 550 and 950 K and has had approximately one monolayer of carbon deposited on it at ~1000 K. It is apparent, therefore, that the original crystallography of the $(VO)_2P_2O_7$ catalyst will not exist during this selective oxidation and that theories that relate selectivity in partial oxidation to the (100) face of the $(VO)_2P_2O_7$ catalyst cannot apply in this case.

Key Words: **partial oxidation; vanadyl pyrophosphate catalyst; *n*-butane; kinetics; mechanism; adsorption.**

INTRODUCTION

Selectivities (product formed/reactant consumed) of the order of 60–80% are routinely achieved in the partial oxidation of hydrocarbons (benzene, *n*-butane, butenes, etc.) over vanadium-based catalysts. The origin of these selectivities has been the subject of considerable investigation and of consequent debate (1–10, 17–20).

In the partial oxidation of benzene to maleic anhydride over VO_2O_5/MoO_3 (3 : 1) catalyst, it has been argued that the selective reactive pathway occurred when an electronically perturbed oxygen molecule (an O_2^- species produced by the molecular oxygen chemisorbing on a V^{4+} site forming an $O_2^-V^{5+}$ dimer) added para across the electronically perturbed benzene ring. This is produced when the benzene molecule adsorbes on a V^{5+} site giving a $C_6H_6^+V^{4+}$ dimer (1, 2). Orbital symmetry conservation arguments showed this to be an allowed reaction (3). The adduct (adduct 1) so obtained is

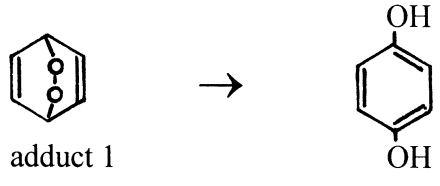

adduct 1

and was thought to rearrange to hydroquinone, which after an identical para addition of O_2^- and rearrangement produced maleic anhydride. Subsequent quantum mechanical calculations by Haber and co-workers showed this to be a feasible low-energy pathway (4, 5). The fundamental thesis of these papers was that reaction of the benzene with the oxygen ions of the V_2O_5/MoO_3 lattice would probably be unspecific and lead to the formation of CO and CO_2.

However, a considerable body of opinion holds that it is the oxygen of the catalyst that is the oxidant and that selectivity to maleic anhydride derives from the configuration of the adsorbate imposed on it by the crystal field of the oxide. In the case of the oxidation of *n*-butane to maleic anhydride over a vanadium pyrophosphate catalyst, it is the (100) face of that catalyst that is though to be selective by its imposition of a *maleic anhydride-like* configuration on the adsorbed butane (6–10) (Fig. 1).

The mechanism is essentially Mars and Van Krevelen, in which the gas phase oxygen is used to replace the catalyst (11). Recently it has been reported that the anaerobic

0021-9517/00 $35.00

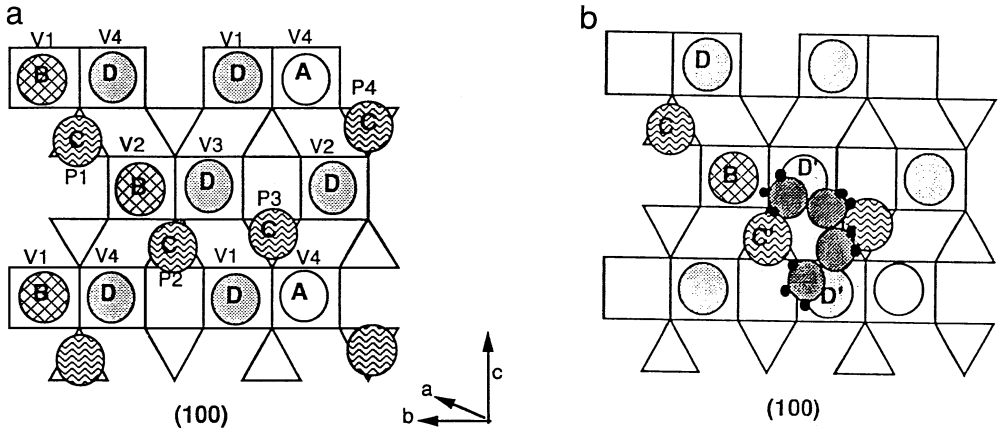

FIG. 1. (a) Plan of the oxygen atoms/ions on the (100) face of $(VO)_2P_2O_7$. The oxygens A, B, and D are bonded to vanadium and the oxygen C is bonded to phosphorus. They are of increasing activity A to D. (b) Postulated configuration of the *n*-butane adsorbed on the oxygen atoms/ions on the (100) face of $(VO)_2P_2O_7$ (6–10).

oxidation of *n*-butane over a vanadium pyrophosphate catalyst produced selectivities of ~80%. These selectivities are roughly 10–20% higher than those achieved in aerobic oxidation (12). The observation has found application industrially in a plant in which the *n*-butane is oxidized anaerobically in one part of the reactor system, after which the oxygen-depleted catalyst is transferred to another reactor for reoxidation (13). The existence of this process would appear to eliminate chemisorbed oxygen as the oxidant; indeed, the fact that ~1–2% of the total oxygen content of the catalyst is used (14), corresponding to more than monolayer coverage of chemisorbed oxygen, effectively rules out the involvement of chemisorbed oxygen.

This paper is part of a study to investigate the origins of selectivity in the anaerobic oxidation of *n*-butane to maleic anhydride. The nature of the chemisorption of *n*-butane on the $(VO)_2P_2O_7$ surface has been determined by temperature-programmed desorption and temperature-programmed reaction spectroscopy, techniques that have allowed: (i) evaluation of the adsorption and desorption activation energies of the adsorption process, (ii) explicit definition of the structure of adsorbate on the oxide surface, and (iii) determination of the surface coverage of that adsorbate. The mechanism of the selective oxidation has been elucidated by anaerobic temperature-programmed reaction.

EXPERIMENTAL

Catalyst Preparation

The catalyst, vanadyl pyrophosphate, $(VO)_2P_2O_7$ with $P:V = 1.03$, was prepared in organic medium. Vanadium pentoxide (15.00 g from Sigma) was suspended by rapid stirring into isobutyl alcohol (90 cm^3) and benzyl alcohol (60 cm^3). The vanadium oxide–alcohol mixture was refluxed for 3 h at 393 K under continuous stirring. During this period the solution changed in color from brown to black. The mixture was then cooled to room temperature and left stirring at this temperature overnight. *Ortho*-phosphorus acid (99%) was added in such quantity as to obtained a final P : V atomic ratio of 1.03. The resulting solution was again heated to 393 K and maintained under reflux with constant stirring for 2 h. During this time, a reduced vanadium phosphate was formed, as indicated by a change in color from black to blue. Then the slurry was filtered, washed, and dried at 423 K. Figure 2a is the x-ray powder diffraction pattern (obtained on a Scintag XDS200) of the material produced showing the main peaks at 2θ values of 15.6°, 19.7°, 24.3°, 27.1°, and 30.4°, all of which are consistent with the material being crystalline $VOHPO_4 \cdot 0.5H_2O$ (14–18).

This vanadyl hydrogen phosphate hemihydrate precursor was then calcined in air for 6 h at 673 K followed by an additional 3 h at the same temperature in a *n*-butane/air mixture (0.75% *n*-butane, 25 $cm^3\ min^{-1}$). Figure 2b is the XRD pattern of this material showing the main peaks at 2θ value of 22.7°, 28.4°, and 28.9°, consistent with material being crystalline $(VO)_2P_2O_7$. This material is quite different from the *poorly crystalline* VPO catalysts obtained by Kiely and co-workers after treating the vanadyl hydrogen phosphate hemihydrate for different periods of time in a *n*-butane/oxygen helium mixture (1.6, 18, and 80.4%) at 40 $cm^3\ min^{-1}$ (19). This could be due to their higher butane partial pressure, lower oxygen partial pressure, and higher flow rate producing a more defective material.

Figure 3 (curve a) is the diffuse reflectance infrared Fourier transform spectrum (DRIFTS) obtained on a Nicolet Magna 550 infrared spectrometer for the $VOHPO_4 \cdot 0.5H_2O$ material; Fig. 3 (curve b) is the DRIFTS spectrum of the $(VO)_2P_2O_7$ material. Table 1 lists their absorption bands and putative assignments. They are corroborative evidence

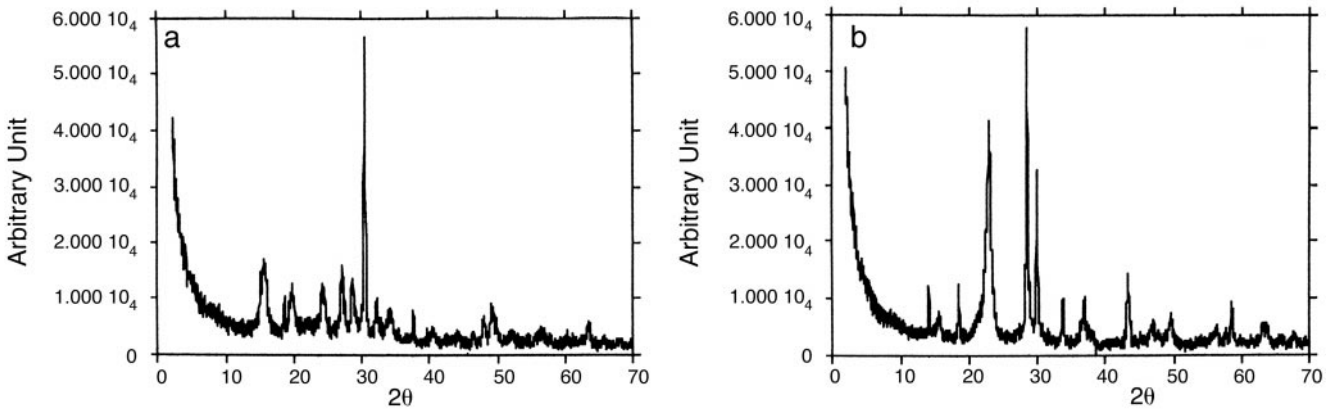

FIG. 2. (a) X-ray diffraction pattern of the precursor identifying it as $VOHPO_4 \cdot 0.5H_2O$. (b) X-ray diffraction pattern of the material produced by treating the hemihydrate precursor in air at 673 K for 6 h followed by an additional 3 h in *n*-butane/air (0.75% *n*-butane) also at 673 K, identifying it as $(VO)_2P_2O_7$.

for the material in curve a being the hemihydrate and that in curve b being vanadyl pyrophosphate (14–18, 20–22).

The surface area of the vanadyl pyrophosphate was measured *in situ* by N_2 adsorption at 77 K to be $\sim$24 $m^2\ g^{-1}$. It should be pointed out that the *n*-butane/air pretreatment for 3 h used here is only half the time used by Trifiro and co-workers to produce their most selective morphology of the vanadyl pyrophosphate-based catalyst (23).

The Gases

Helium (ECM) was 99.995% pure and was passed through an Oxyclear catalyst before use to remove trace quantities of oxygen. Oxygen was supplied both by BOC and ECM. The *n*-butane helium mixture (1.85% in helium) was supplied by BOC; all was 99.995% pure and was used direct from the cylinder.

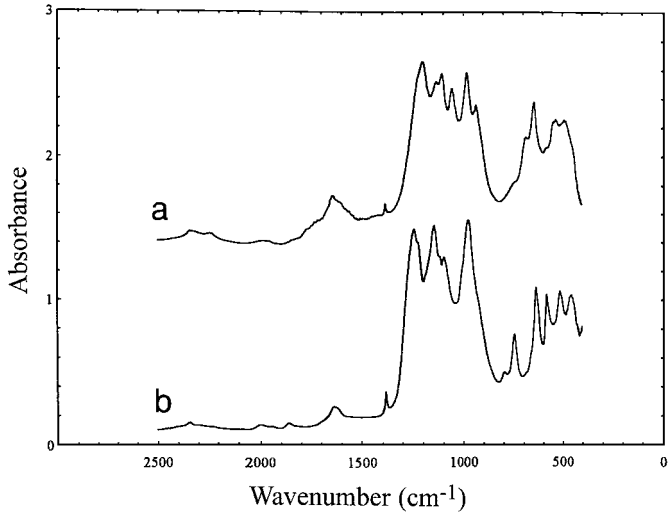

FIG. 3. Curve (a) is the infrared spectrum of the hemihydrate precursor. Curve b is the infrared spectrum of $(VO)_2P_2O_7$.

The Apparatus

The continuous flow multipurpose microreactor system used to conduct total surface area (TSA), temperature-programmed desorption (TPD), temperature-programmed reaction (TPRn), and temperature-programmed oxidation (TPO) experiments has been described previously (24, 25). It is a single-tube reactor (20 cm long, 0.4 cm i.d.) connected via a heated capillary to a quadrupole mass spectrometer (Hiden Analytical, Warrington, England) that is capable of monitoring 16 masses continuously with temperature/time. The catalyst, in the form of powder (0.50 g), was placed in the reactor and could be cooled to 77 K by pumping liquid nitrogen around it for the TSA measurements or heated by an electrical furnace to 1100 K. A thermocouple was embedded in the center of the catalyst to allow accurate temperature readings to be obtained. The temperature of

TABLE 1

Infrared Spectra of $VOHPO_4 \cdot 0.5H_2O$ and $(VO)_2P_2O_7$ Adsorption Bands (cm^{-1}) and Vibration Assignments

$VOHPO_4 \cdot 0.5H_2O$		$(VO)_2P_2O_7$	
Adsorption band	Assignment	Adsorption band	Assignment
1199	$\nu_{as}(PO_2)$	1240	}
1134	δ_{ip}(P–OH)	1220	}
1105	}	1144	}$\nu(PO_3)$
1056	}$\nu(PO_3)$	1117	}
982	ν(V=O)	1096	}
934	ν(P–OH)	972	ν(V=O)
686	$\omega(H_2O)$	797	ν[V–(O=V)
645	δ(P–OH)	746	ν_s(P–O–P)
548	}	635	$\delta_{as}(PO_3)$
535	}δ(OPO)	582	}
490	}	514	$\delta(PO_3)$
		459	}

the reactor was controlled in the temperature-programmed mode by a Newtronics controller. All of the experiments (TSA, TPD, TPRn, TPO) were carried out *in situ* in a completely sealed reactor system.

RESULTS AND DISCUSSION

Oxygen Desorption

The oxygen desorption spectrum shown in Fig. 4 was obtained by pretreating the $(VO)_2P_2O_7$ catalyst by heating it to 673 K in an oxygen flow (101 kPa, 25 cm^3 min^{-1}) and holding it under that flow at 673 K for 1 h before cooling it to 77 K. This high-temperature pretreatment in flowing oxygen removed any last traces of water from the system; since this pretreatment preceded each experiment and since the gases were 99.995% pure, no adventitious dosing of water or any other compound occurred. In addition since we have previously shown that N_2O oxidation of a highly reduced $(VO)_2P_2O_7$ catalyst produced by reduction in CO completely replaces all of the anion defects (26), this oxygen pretreatment is likely to produce a near defect-free $(VO)_2P_2O_7$ material.

Having dosed on the oxygen, the flow was then switched to helium (101 kPa, 25 cm^3 min^{-1}) and the temperature was raised (10 K min^{-1}) to 1100 K following the $m/z = 32$ signal on the mass spectrometer. Peaks are observed at 83, 91, and 1023 K with a shoulder at 998 K. The peaks at 83 and 91 K correspond to desorption activation energies of 23 and 25 kJ mol^{-1}. This is physisorbed oxygen. These values are obtained by solution of the Redhead equation

$$\frac{E_d}{RT_m^2} = \frac{A^{-E_d/RT_m}}{\beta}, \qquad [1]$$

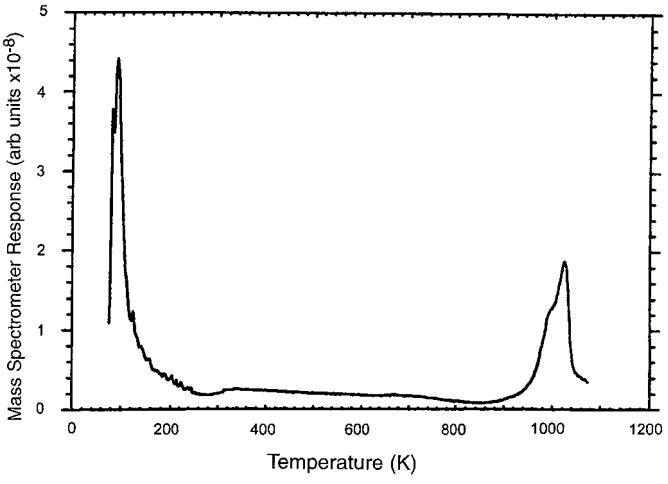

FIG. 4. The temperature-programmed desorption spectrum of oxygen from the $(VO)_2P_2O_7$ catalyst.

where E_d (J mol^{-1}) is the desorption activation energy, T_m (K) is the peak maximum temperature, R (J mol^{-1} K^{-1}) is the gas constant, A (s^{-1}) is the desorption preexponential term, and β (K s^{-1}) is the heating rate, for an assumed value of 10^{13} s^{-1} for the desorption preexponential term (27).

There are no sharp desorption peaks for oxygen in the temperature range 300 to 850 K corresponding to specific sites for chemisorbed molecular oxygen. There is however a broad hump in this range that might derive from the desorption of oxygen from surface oxide states. The shoulder at 998 K and the peak at 1023 K correspond to desorption activation energies of 256 and 282 kJ mol^{-1}. The total amount of oxygen desorbed between 900 to 1100 K is 2.2×10^{20} atoms g^{-1}, which on a catalyst whose surface area is 24 m^2 g^{-1} would correspond to a coverage of 9.2×10^{14} atoms cm^{-2}. Assuming there are approximately 10^{15} atoms cm^{-2} on the surface of the $(VO)_2P_2O_7$ catalyst and that the proportion of oxygen ions on the surface is roughly stoichiometric, then the surface oxygen ion population is 6.9×10^{14} ions cm^{-2} and so a coverage of 9.2×10^{14} atoms/ions cm^{-2} would correspond to more than a monolayer of chemisorbed oxygen. It is therefore lattice oxygen, the total amount desorbing being ~1% of the lattice oxygen. This is approximately the amount of oxygen involved in the industrial anaerobic oxidation of *n*-butane over the $(VO)_2P_2O_7$ catalyst (9).

The Adsorption of n-Butane at 223 K

The vanadyl phosphate catalyst was pretreated in oxygen (25 cm^3 min^{-1}, 1 h, 101 kPa) at 673 K after which the temperature was lowered to 223 K under the oxygen flow. The flow was then switched to a *n*-butane He stream (1.85% butane, 101 kPa, 25 cm^3 min^{-1}) that was passed over the catalyst for 30 min. No CO, CO_2, H_2O, or any other partially oxidized product, e.g., butene, butadiene, was observed during the dosing of the *n*-butane onto the catalyst at 223 K. Having dosed the *n*-butane on for 30 min at 223 K, the flow was switched to helium (25 cm^{-3}, 101 kPa) for 30 min at 223 K, during which time no detectable species (CO, CO_2, H_2O, butene, butadiene, or *n*-butane) desorbed from the catalyst. Temperature programming was begun at the end of the 30-min He flow, producing the desorption profile shown in Fig. 5.

Now, in addition to the oxygen seen in Fig. 4, water, carbon dioxide, carbon monoxide, and *n*-butane are also observed in the desorption profile. A complete listing of the amounts of species desorbed and of their peak maximum temperatures is given in Table 2. The oxygen evolves at a peak maximum temperature of 970 K; this is the lattice oxygen seen in Fig. 4.

Water evolves at two peak maxima (370 and 800 K); carbon dioxide and carbon monoxide evolve coincidently at a peak maximum temperature of 970 K, the temperature at which the oxygen evolves from the lattice. A small

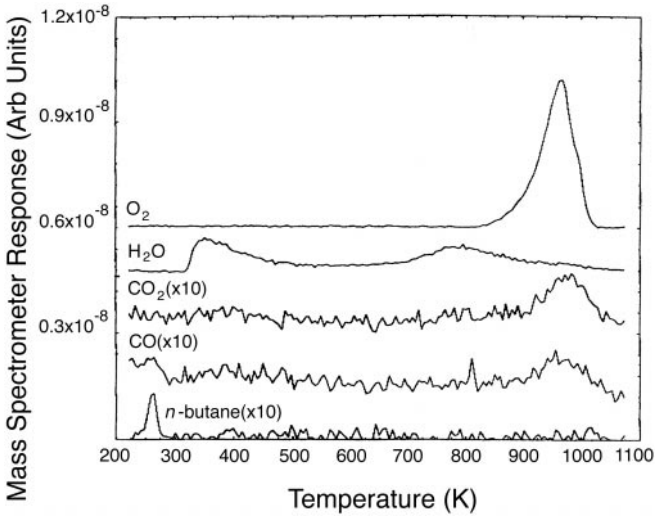

FIG. 5. The temperature-programmed desorption spectrum obtained after having adsorbed *n*-butane at 223 K on the $(VO)_2P_2O_7$ catalyst.

quantity of *n*-butane evolves at a peak maximum temperature of 260 K.

From these observations the adsorption process can be described by the following elementary reactions:

1. $C_4H_{10(g)} + O_{(s)} \rightleftharpoons C_4H_{9(a)} + OH_{(a)}$
2. $OH_{(a)} + OH_{(a)} \rightleftharpoons H_2O_{(g)} + O_{(s)} + Vo_{(s)}$
3. $C_4H_{9(a)} + 4\frac{1}{2}O_{(s)} \rightarrow 4\frac{1}{2}H_2O_{(g)} + 4C_{(a)}$
4. $4C_{(a)} + 6O_{(l)} \rightarrow 2CO_{(g)} + 2CO_{2(g)} + 6Vo_{(l)}$
5. $O_{(l)} \rightleftharpoons \frac{1}{2}O_{2(g)} + Vo_{(l)}$,

where the subscripts (g), (a), and (l) refer to gas phase, adsorbed species, and lattice species; Vo(l) is a lattice oxygen vacancy.

TABLE 2

Amounts of Species Desorbed upon Temperature Programming following *n*-Butane Adsorption on the $(VO)_2P_2O_7$ Catalyst at 223 K

Species	Peak maximum temperature (K)	Amount desorbed (molecules g^{-1})
H_2O	340	4.1×10^{19}
H_2O	790	4.2×10^{19}
CO_2	970	4.2×10^{19}
CO	950	7.7×10^{18}
O_2	950	2.4×10^{20}
C_4H_{10}	260	4.6×10^{17}

Note. Total carbon $(CO + CO_2) = 5.0 \times 10^{19}$ C atoms g^{-1}
$= 2.1 \times 10^{14}$ C atoms cm^{-2}
or a C_4 coverage of 5×10^{13} butyl species cm^{-2}. Total H_2O is 8.3×10^{19} molecules g^{-1}. The surface carbon calculated from the water evolved assuming a H_2 : C ratio of 1.25 in *n*-butane is 6.6×10^{19} C atoms g^{-1}.

It is clear that from these results even at an adsorption temperature of 223 K the adsorption of *n*-butane is dissociative, forming *n*-butyl and hydroxyl species (reaction 1). Some of the water that evolves at the peak maximum temperatures of 370 and 800 K derives from this; the majority of the water, however, as will be explained below, results from the oxidative dehydrogenation of the adsorbed butyl species (the composite reaction 3). These two water peaks show that the $O_{(s)}$ species are of different strength of binding at the surface. While it is possible that this surface migration of the hydroxy groups from the butyl–hydroxyl pair occurs during the 30-min dosing period of the *n*-butane at 223 K, it is more likely that the surface migration is activated and that it occurs upon heating from 223 to 260 K. At 260 K the hydrogen atoms of those hydroxyl species that have not migrated from the original adsorption site recombine with the *n*-butyl species, producing butane in the gas phase.

Several additional conclusions can be drawn from this desorption profile. They are:

(i) The activation energy for the migration of the surface hydroxyl species is low so that under steady state operating temperatures (between 600 to 700 K) they will be highly mobile on the surface, affording little prospect of the *n*-butyl species and the hydrogen atom of the hydroxy species recombining under steady state conditions. The adsorption of *n*-butane therefore is essentially irreversible.

(ii) The recombinative desorption activation of the *n*-butyl–hydroxyl pair, calculated from the Redhead equation (Eq. [1]), for the assumed value of 10^{13} s^{-1} for the desorption preexponential term, is 72 kJ mol^{-1}. The surface residence time, τ, of an adsorbate at any temperature, T, can be calculated by use of the Frenkel equation

$$\tau = \frac{e^{\Delta H/RT}}{A},$$

where τ is the residence time (s), ΔH is the heat of adsorption (J mol^{-1}), and R is the gas constant (8.314 J K^{-1} mol^{-1}). For the residence time of any adsorbate to exceed the 30 min He purge time at 223 K, the heat of adsorption must exceed 69 kJ mol^{-1}. The desorption activation energy of 72 kJ mol^{-1} for butane obtained from the Redhead equation easily exceeds this value.

(iii) Since no water is evolved during the adsorption of the *n*-butane, the ionic configuration of the $(VO)_2P_2O_7$ surface is essentially unchanged and so this result shows that the adsorbed butyl species is not forced by the crystal field of the $(VO)_2P_2O_7$ lattice into a structure that predisposes it to be oxidized to maleic anhydride as has been suggested (6, 9).

(iv) The surface O species on the $(VO)_2P_2O_7$ catalyst abstract the hydrogen atoms from the adsorbed butyl species leaving carbon on the surface. The residual carbon is oxidized to CO_2 by the lattice oxygen species as they emerge

at ~1000 K. The purpose of the 6-h activation process in butane/air at 673 K used to produce the highly selective morphology (23) may be to remove these active unselective oxygen species.

The total amount of water evolved is 8.3×10^{19} molecules/g (catalyst) in two peaks of roughly equal amounts. Since each water molecule corresponds to the removal of one oxygen atom from the surface of the catalyst, on the basis of a surface area of 24 $m^2\ g^{-1}$, this corresponds to the removal of 3.4×10^{14} oxygen atoms cm^{-2}. Taking the oxygen atom/ion population to be 6.9×10^{14} species cm^{-2} as explained previously, the reaction of the hydrogen atoms of the adsorbed butyl species has removed approximately 50% of the surface oxygen ions as atoms. This is consistent with the idea that activation in butane/air mixtures at 673 K for 6 h removes the more active unselective surface oxygen species.

The butyl surface coverage calculated from the number of hydrogen atoms in the evolved water is 6.9×10^{13} species per cm^2. The butane desorbed at 260 K corresponded to a coverage of 1.9×10^{12} molecule cm^{-2} so that the majority of the hydroxyl species formed by the dissociative adsorption of the *n*-butane appear to have migrated from the original adsorption site.

Carbon dioxide (4.2×10^{19} molecules g^{-1}) and carbon monoxide (7.7×10^{18} molecules g^{-1}) are evolved roughly coincidentally at ~1000 K, i.e., the temperature at which the oxygen evolves from the lattice. No water is evolved at this temperature and so the surface oxygen species of the $(VO)_2P_2O_7$ catalyst appear to have completely dehydrogenated the adsorbed butyl species before this temperature. The total carbon coverage is 5.0×10^{19} C atom g^{-1}. This would predict a surface butyl coverage of 5.2×10^{13} butyl species cm^{-2} which is only slightly lower than that predicted from the amount of water evolved. These results however confirm that the adsorbate is the C_4H_9 butyl–hydroxyl pair.

The Adsorption of n-Butane at 423 K

The catalyst pretreatment prior to the adsorption of *n*-butane at 423 K was identical to that adopted for the pretreatment prior to the adsorption of *n*-butane at 223 K. The *n*-butane was dosed onto the catalyst at 423 K from the *n*-butane/He stream (1.85% *n*-butane, 101 kPa, 25 $cm^3\ min^{-1}$) for 30 min. The temperature was then lowered to 223 K under the *n*-butane/He stream at which point the catalyst was flushed with He for 30 min before raising the temperature to 1123 K under that stream. The desorption profile so obtained is shown in Fig. 6.

In contrast to what was observed upon dosing the *n*-butane onto the $(VO)_2P_2O_7$ catalyst at 223 K, dosing the *n*-butane on at 423 K resulted in the production of an unquantified amount of H_2O in the gas phase during the dosing. In addition, again in contrast to what was observed at 223 K, the desorption spectrum obtained after dosing at 423 K did not include any *n*-butane desorption. The only molecules observed were H_2O, CO_2, CO, and O_2. No selective oxidation products, e.g., butene or butadiene, were observed. Therefore during the adsorption of the *n*-butane and the formation of the butyl–hydroxyl pair, the hydroxyl species diffuses away from the butyl species completely (possibly forming the H_2O which was observed in the gas phase at that point) while the configuration of the remaining adsorbed *n*-butyl species on the $(VO)_2P_2O_7$ catalyst is not constrained by the crystal field of the catalyst to be selectively oxidized to maleic anhydride (A complete listing of the amounts of species evolved and of their peak maximum temperatures is given in Table 3).

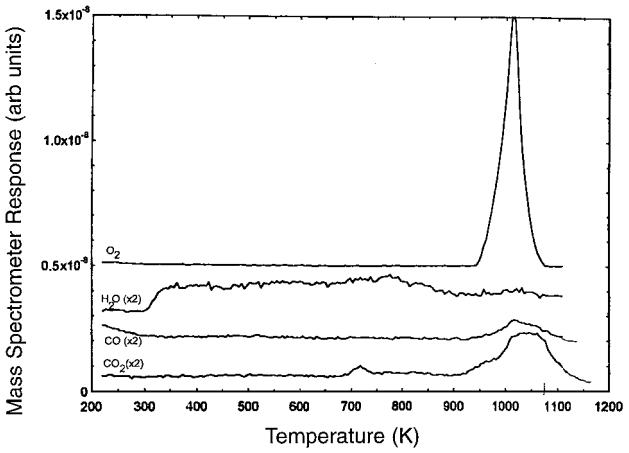

FIG. 6. The temperature-programmed desorption spectrum obtained after having adsorbed *n*-butane at 423 K on the $(VO)_2P_2O_7$ catalyst.

Water is evolved at a roughly constant rate in the temperature range 330 to 775 K, the total amount being 5.9×10^{19} molecules/g catalyst, which is slightly smaller than that evolved (8.3×10^{19} molecules/g catalyst) having adsorbed the *n*-butane at 223 K. This, however, does not take account

TABLE 3

Amounts of Species Desorbed upon Temperature Programming following *n*-Butane of Adsorption on the $(VO)_2P_2O_7$ Catalyst at 423 K

Species	Peak maximum temperature (K)	Amount desorbed (molecules g^{-1})
H_2O	No clear maximum	5.9×10^{19}
CO_2	1042	3.4×10^{19}
CO	1018	5.8×10^{18}
O_2	1013	3.2×10^{20}

Note. Total carbon ($CO + CO_2$) $= 4.0 \times 10^{19}$ C atoms g^{-1} $\equiv 1.7 \times 10^{14}$ C atoms cm^{-2}.

The surface carbon calculated from the water evolved assuming a H_2 : C ratio of 1.25 in *n*-butane is 4.8×10^{19} C atoms g^{-1}.

of the unquantified amount of water evolved during adsorption at 423 K. Since the water is produced by the dehydrogenation of the adsorbing *n*-butane species, it appears therefore that the adsorption of *n*-butane in the *n*-butyl–hydroxyl dimer form is not, or is only mildly, activated. Again the broad range of temperature in which the water is evolved upon temperature programming reflects the range of activities of the surface oxygen atoms.

As before, the oxygen evolving from the lattice at ~1000 K oxidizes the adsorbed carbon that was produced by the dehydrogenation of the adsorbed butyl species. The sum of the CO and CO_2 produced corresponds to 4.5×10^{19} atoms/g catalyst or a coverage of 1.9×10^{14} C atoms/cm^2 ~20% of a monolayer or a butyl species coverage of 5×10^{13} species cm^{-2}. Assuming that the water evolution 5.9×10^{19} molecules/g catalyst results from the dehydrogenation of the adsorbed butyl species, the amount of water produced would predict a carbon atom coverage of 4.8×10^{19} C atoms/g catalyst. This is in accordance with the carbon atom coverage calculated from the sum of the CO and CO_2 produced by oxidation of the surface carbon by the lattice oxygen, confirming that the adsorbate is a butyl species and that the adsorbed butyl species is completely dehydrogenated by the surface oxygen atoms, the residual carbon being completely oxidized by the lattice oxygen.

Anaerobic Temperature-Programmed Reaction of the n-Butane/He (1.85% n-Butane) Stream over the $(VO)_2P_2O_7$ Catalyst

Figure 7 is the temperature-programmed reaction profile obtained by passing a *n*-butane/He stream (1.85% butane, 101 kPa, 25 cm^3, min^{-1}) over the $(VO)_2P_2O_7$ catalyst that had been preoxidized in O_2 at 673 K for 1 h. With the catalyst oxidized, the temperature was lowered to ambient under the oxygen stream before being switched to the *n*-butane/He stream and raising the temperature at 5 K min^{-1}. A complete listing of the amounts of species evolved and of their peak maximum temperatures is given in Table 4. This profile is complex.

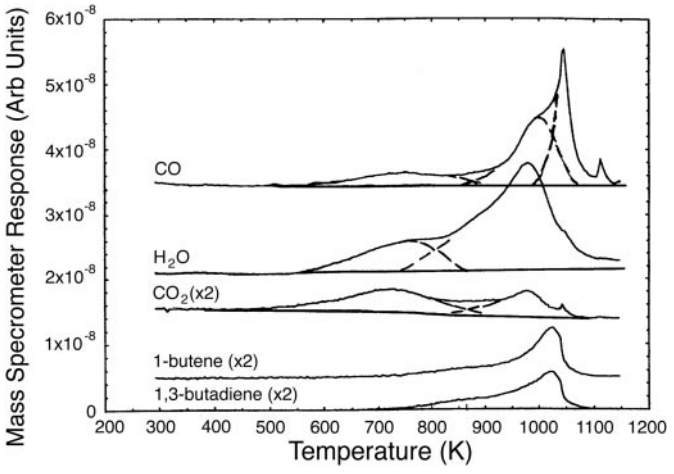

FIG. 7. The anaerobic temperature-programmed reaction profile of *n*-butane (1.85% in He) over the $(VO)_2P_2O_7$ catalyst.

TABLE 4

Amounts of Species Evolved on Anaerobic Temperature Programmed Reaction of a *n*-Butane/He Mixture (1.85% *n*-butane) over the $(VO)_2P_2O_7$ Catalyst

Species	Peak maximum temperature (K)	Amount evolved (molecules g^{-1})
CO	730	3.5×10^{19}
CO	1000	1×10^{20}
CO	1040	1×10^{20}
CO_2	730	15.5×10^{19}
CO_2	960	4.8×10^{19}
H_2O	730	2.2×10^{20}
H_2O	960	7.2×10^{20}

Note. Total carbon evolved at 730 K ($CO + CO_2$) $= 3.5 \times 10^{19} + 15.5 \times 10^{19} = 1.9 \times 10^{20}$ C atoms g^{-1}. Total predicted surface carbon from the amount of water evolved at 730 K assuming a H_2 : C ratio of 1.13 in butyl is 1.8×10^{20} C atoms g^{-1}. Total carbon evolved at 960 K ($CO + CO_2$) $= 1 \times 10^{20} + 0.5 \times 10^{20} = 1.5 \times 10^{20}$ C atoms g^{-1}. Total predicted surface carbon from the amount of water evolved at 960 K assuming a H_2 : C ratio of 1.13 in butyl is 5.8×10^{20} C atoms g^{-1}. Therefore the carbon deposited on the surface is 4.3×10^{20} C atoms g^{-1} or 1.8×10^{15} C atoms cm^{-2}.

Water (2.2×10^{20} molecules g^{-1}), CO (3.5×10^{19} molecules g^{-1}), and CO_2 (1.55×10^{20} molecules g^{-1}) are evolved coincidently at a peak maximum temperature of 730 K. This corresponds to a C : H ratio of 1 : 2.3, which is exactly the C : H ratio of a butyl species. This peak therefore derives from the complete oxidation of an adsorbed butyl species. The amount of butyl species adsorbed calculated from the amount of H_2O or the sum of the CO and CO_2 evolved is 4.1×10^{20} species/g or a coverage of 2×10^{14} butyl species cm^{-1}. Were the butyl species to be adsorbed end-on, this would correspond to roughly 20% of a monolayer. This value is roughly the surface population of the protruding oxygen atoms of the vanadyl (V=O) species, which might implicate these in the initial adsorption step.

The difference in the oxidative behavior of the butyl species produced by adsorption in the temperature-programmed reaction mode compared with that of those produced by isothermal adsorption at 423 or 223 K (the latter were completely dehydrogenated before the carbon was oxidized (Figs. 5 and 6), whereas in the temperature-programmed reaction mode the C and the H of the butyl species were oxidized simultaneously (Fig. 7)), could derive from the cooling of the lower coverage of butyl species (~5×10^{13} butyl species cm^{-2}) adsorbed at 423 to 223 K, or adsorbing at 223 K, allowing the butyl species that had been adsorbed initially end-on to lie flat on the surface

and so to become hydrogen bonded to the oxygen ions on the $(VO)_2P_2O_7$ surface. Complete initial dehydrogenation therefore would then be inevitable. In the temperature-programmed reaction, the end-on bonded butyl species is simply oxidized sequentially in CH_3 and CH_2 units, producing CO, CO_2, and H_2O coincidentally.

The total amount of oxygen removed from the $(VO)_2P_2O_7$ catalyst during the oxidation of this 730 K butyl species was 1.7×10^{15} O ions cm^{-2}. Since the oxygen ion surface population is approximately 6.9×10^{14} ions cm^{-2}, oxidation of the butyl species removes at least two monolayers of oxygen from the lattice of the $(VO)_2P_2O_7$ catalyst. This enormous loss of oxygen will probably be accommodated by the $(VO)_2P_2O_7$ catalyst by the creation of a large number of shear planes (28), creation of which will still allow some of the original crystallography to exist. Water (7.2×10^{20} molecules g^{-1}) and CO_2 (4.8×10^{19} molecules g^{-1}) are evolved at a peak maximum temperature of 960 K with CO (1×10^{20} molecules g^{-1}) evolving at the slightly higher temperature of 1000 K. The C : H ratio of this peak is 1 : 9.6; even when the higher temperature (1040 K) CO evolving state (1×10^{20} molecules g^{-1}) is taken into account this reduces the ratio only to 1 : 5.8. The surface is therefore becoming carbided. The difference between the amount of carbon predicted to be deposited from the water evolved, i.e.,

$$\left(\frac{H_2O \times 2}{10}\right) \times 4 = 7.2 \times 10^{20} \times 0.8 \text{ or}$$

$$5.76 \times 10^{20} \text{ C atoms } g^{-1},$$

and that removed as CO and CO_2 ($2 \times 10^{20} + 4.8 \times 10^{19} = 2.5 \times 10^{19}$ atoms g^{-1}) is 3.26×10^{20} atoms/g^{-1} or a carbon atom coverage of 1.4×10^{15} atoms cm^{-2}. This is more than monolayer coverage.

It can be seen from Figs. 4, 5, and 6 that oxygen evolution/desorption from the $(VO)_2P_2O_7$ lattice occurs between 830 and 1070 K. No oxygen evolution is observed here. In addition to the CO, CO_2, and H_2O being produced in this temperature range, the anaerobic oxidation of *n*-butane produces butene (identified using the $m/z = 41$ fragment which is unique to butene) and but-1,3-diene (identified using the $m/z = 39$ and 54 fragments both of which have only minor contributions from *n*-butane and butene). The butene and butadiene profiles are shown in detail in Fig. 8, which shows clearly, by the fact that the butadiene peak is not a constant fraction of the butene peak and indeed in the lower temperature range is higher than the butene peak, that they are both genuine selective products of the reaction. The amount of butene produced is 1.2×10^{20} molecule g^{-1} and of butadiene is 0.9×10^{20} molecule g^{-1}. The reactions involved are

$$n\text{-}C_4H_{10} + O_{(l)} \rightarrow C_4H_8 + H_2O$$

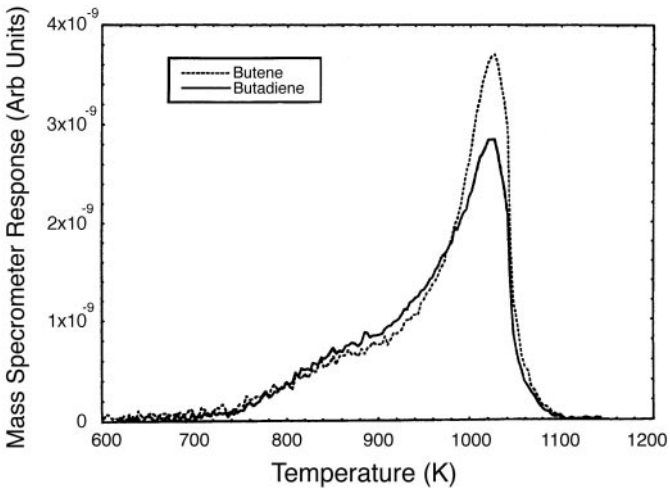

FIG. 8. The temperature dependence of the rate of production of butene and butadiene in the anaerobic temperature-programmed reaction of *n*-butane over the $(VO)_2P_2O_7$ catalyst.

and

$$n\text{-}C_4H_{10} + 2O_{(l)} \rightarrow C_4H_6 + 2H_2O,$$

where $O_{(l)}$ is the lattice oxygen.

The amount of oxygen required for their production is 3.0×10^{20} atoms g^{-1}. This is roughly the same as the amount of oxygen evolving from the lattice upon temperature programming in He (Fig. 4). Furthermore the peak maximum temperature of the oxygen evolution 1020 K coincides with that of the butene and butadiene evolution while the temperature dependence of the production of the butene and butadiene closely resembles that of the oxygen evolution of Fig. 1 and is quite different from the temperature dependence of CO, CO_2, or H_2O. This suggests that it is the oxygen that evolves from the lattice in the desorption state at 1020 K that is responsible for the selective oxidation of *n*-butane to butene and butadiene. Other forms of *surface* oxygen, bearing in mind that at least two monolayers of this oxygen have been shown to be involved, appear to be unselective. The surface of the operating catalyst producing butene and butadiene at 1020 K will be considerably different from the crystalline form of the $(VO)_2P_2O_7$ lattice that was loaded into the reactor. It has lost at least two monolayers of surface oxygen and has approximately a monolayer or more of carbon deposited on it.

The fact that selective oxidation occurs on this surface when the ~1000 K desorbing oxygen evolves at the surface suggests that one crystal face (possibly a defected form of the (100) face) must be free from carbon and that the oxygen evolution is unique to it. Were carbon deposited on this face, it would have been oxidized to carbon dioxide by the oxygen evolving from the lattice at ~1000 K and so there would be no balance between the amount of oxygen desorbing at that temperature and the amount required for the selective oxidation of *n*-butane to butene and butadiene.

We have shown that the anaerobic temperature-programmed oxidation of but-1,3-diene over the $(VO)_2P_2O_7$ catalyst produces dihydrofuran, furan, and maleic anhydride (29). In unpublished work we have also shown that, in the same type of anaerobic, temperature-programmed oxidation experiment, dihydrofuran and furan produce maleic anhydride using the same lattice oxygen (28). All of these occur on a carbided surface using the oxygen that would have desorbed as molecular oxygen at ~1000 K (30). While it is clear that the intermediate leading to the formation of dihydrofuran, furan, and maleic anhydride must be cyclic, it is difficult to sustain the notion that this is induced by the crystal field of the original $(VO)_2P_2O_7$ lattice (6–9) bearing in mind: (i) the possible disruption of the lattice by the loss of oxygen and (ii) that a butyl species adsorbed flat on the oxide will be immediately dehydrogenated. The mechanism by which the end-on adsorbed butyl-type species are transformed to dihydrofuran and furan is by coiling the other end group onto the oxygen. The importance of the oxygen desorbing at this temperature is that it ejects the cyclic oxygenated products, dihydrofuran or furan, from the surface.

Aerobic Temperature-Programmed Oxidation of n-Butane (0.75% in Air) over the $(VO)_2P_2O_7$ Catalyst

The $(VO)_2P_2O_7$ catalyst was preoxidized in oxygen (25 cm^3 min^{-1}, 101 kPa, 673 K, 1 h) in a fashion identical to that employed in the aerobic temperature-programmed oxidation. Having preoxidized the catalyst, the temperature was lowered to ambient under the oxygen flow before switching to the hydrocarbon/air flow (0.75% *n*-butane in air, 25 cm^3 min^{-1}, 101 kPa) and temperature programming from ambient to 1100 K at 5 K min^{-1}. The temperature dependence of the evolution of the products is shown in Fig. 9.

Comparison with Fig. 7 shows that it is completely different from anaerobic oxidation. Significantly no selective products (butene, butadiene, furan, or maleic anhydride) are formed. Therefore under these conditions of gas phase composition, temperature flow rate, and weight of catalyst, the coadsorbing oxygen totally oxidizes all of the hydrocarbonacious adsorbates, nullifying the effect of the selective lattice oxygen.

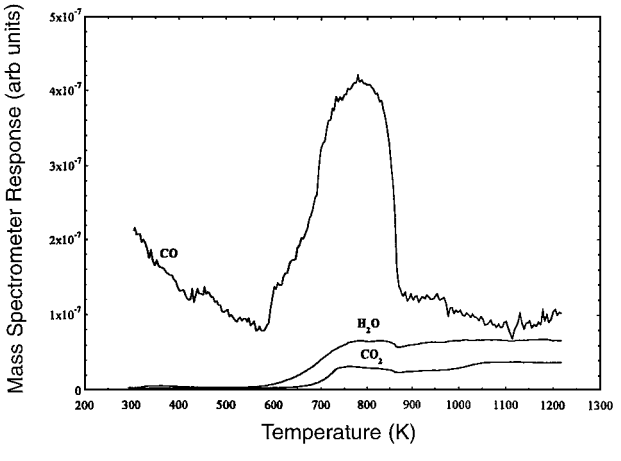

FIG. 9. The aerobic temperature-programmed reaction profile of *n*-butane (0.75% in air) over the $(VO)_2P_2O_7$ catalyst.

CONCLUSIONS

1. *n*-Butane adsorbs at low temperatures (223 and 423 K) as a butyl–hydroxy pair probably on a $V^{5+}O^{2-}$ cation/anion site. The adsorption is negligibly or only mildly activated. At both adsorption temperatures the butyl species lies flat on the surface, becoming completely dehydrogentated by the oxygen ions in the surface layers, the remaining carbon being oxidized to CO and CO_2 at ~1000 K by the lattice oxygen as it emerges from the bulk.

2. In the anaerobic temperature-programmed oxidation of *n*-butane over the $(VO)_2P_2O_7$ catalyst, selective oxidation to butene and butadiene occurs at ~1000 K—the temperature at which oxygen desorbs from the lattice.

3. The total amount of oxygen required for the transient selective oxidation of *n*-butane to butene and butadiene is roughly the same as that which desorbs at ~1000 K, suggesting that this is the selective oxidant.

4. The selective oxidation occurs on a catalyst surface that has lost approximately two monolayers of surface oxygen and has the equivalent of one monolayer of carbon deposited on it. The active face is carbon free. Some of the original crystallography of the $(VO)_2P_2O_7$ catalyst could still exist, the oxygen loss from the catalyst being accommodated for by the formation of extended shear planes.

5. The butyl species adsorbed on the surface during anaerobic temperature-programmed oxidation at higher temperatures (>423 K) appears to be held end-on being oxidized at ~730 K by the oxygen ions in the surface layers of the $(VO)_2P_2O_7$ catalyst to CO, CO_2, and H_2O, which evolve coincidentally. The lattice oxygen evolving at ~1000 K reacts with additional butane adsorbing end-on from the gas phase to form butene and butadiene quantitatively.

6. The amount of oxygen required for the selective oxidation (3×10^{20} atoms/g catalyst) corresponds to roughly two monolayers of oxygen. This oxygen evolves at 1000 K on a catalyst already denuded of surface oxygen.

7. The observation here that the anaerobic oxidation of *n*-butane produces butene and butadiene, only, and not maleic anhydride, suggests that the mechanism of the oxidation of *n*-butane to maleic anhydride is sequential. Corroborative evidence for this conclusion is to be found in our observation that the anaerobic oxidation of but-1-ene produces butadiene and furan while that of but-1,3-diene produces furan and maleic anhydride (9). There appears to be no direct oxidative route to maleic anhydride (10).

8. There being no other oxygen available, the oxygen that evolves from the $(VO)_2P_2O_7$ catalyst at ~1000 K must be the selective oxidant used in the industrial partial oxidation of *n*-butane to maleic anhydride. It will evolve at a slower rate at 650–750 K, the temperature range used industrially (13), compensation for which is made for in the contact times employed which are longer than those used here.

REFERENCES

1. Lucas, J., Vandervell, H. D., and Waugh, K. C., *J. Chem. Soc. Faraday Trans. 1* **77**, 15 (1981).
2. Lucas, J., Vandervell, H. D., and Waugh, K. C., *J. Chem. Soc. Faraday Trans. 1* **77**, 31 (1981).
3. Petts, R. W., and Waugh, K. C., *J. Chem. Soc. Faraday Trans. 1* **78**, 803 (1982).
4. Bielanski, A., and Haber, J., *in* "Oxygen in Catalysis," p. 395. Dekker, New York, 1991.
5. Witko, M., Broclawik, E., and Haber, J., *J. Mol. Catal.* **26**, 249 (1984).
6. Ziolotkowski, J., Bordes, E., and Courtine, P., *J. Catal.* **122**, 126 (1990).
7. Ziolotkowski, J., Bordes, E., and Courtine, P., *Stud. Sci. Surf. Catal.* **55**, 625 (1991).
8. Ziolotkowski, J., Bordes, E., and Courtine, P., *J. Mol. Catal.* **84**, 307 (1993).
9. Bordes, E., *Catal. Today* **16**, 27 (1993).
10. Zhang-Lin, Y., Forrissier, M., Sneeden, R. P., Vedrine, J. C., and Volta, J. C., *J. Catal.* **145**, 256 (1994).
11. Mars, J., and van Krevelen, D. W., *Chem. Eng. Sci., Spec. Suppl.* **3**, 41 (1954).
12. Lerou, J. J., and Mills, Ph., *in* "Precision Process Technology," (M. P. C. Weijnen and A. A. Drinkenburg, Eds.), p. 175. Kluwer Academic, Dordrecht/Norwell, MA, 1993.
13. Lerou, J. J., and Ng, K. M., *Chem. Eng. Sci.* **51**, 1595 (1996).
14. Lerou, J. J., private communication.
15. Batis, N. H., Batis, H., Ghorbel, A., Vedrine, J. C., and Volta, J. C., *J. Catal.* **128**, 248 (1991).
16. Granados, M. L., Conesa, J. C., and Fernandez-Garcia, M., *J. Catal.* **141**, 671 (1993).
17. Igarashi, H., Tsuji, K., Okuhara, T., and Misono, M., *J. Phys. Chem.* **97**, 7065 (1993).
18. Johnson, J. W., Johnston, D. C., Jacobson, A. J., and Brody, J. F., *J. Am. Chem. Soc.* **106**, 8123 (1984).
19. Kiely, C. J., Burrows, A., Hutchings, G. J., Bere, K. E., Volta, J.-C., and Abon, M., *Faraday Discuss. R. Soc. Chem.* **105**, 103 (1996).
20. Wenig, R. W., and Schrader, G. C., *Ind. Eng. Chem. Fundam.* **25**, 612 (1986).
21. Busca, G., Cavani, F., Centi, G., and Trifiró, F., *J. Catal.* **99**, 400 (1986).
22. Bordes, E., and Courtine, P., *J. Catal.* **57**, 236 (1979).
23. Busca, G., Centi, G., Trifiro, F., and Lorenzelli, V., *J. Phys Chem.* **90**, 1337 (1986).
24. Chinchen, G. C., Hay, C. M., Vandervell, H. D., and Waugh, K. C., *J. Catal.* **103**, 79 (1987).
25. Waugh, K. C., *Appl. Catal.* **43**, 315 (1988).
26. Taufiq-Yap, Y. H., Sakakini, B. H., and Waugh, K. C., *Catal. Lett.* **48**, 105 (1997).
27. Redhead, P. A., *Vacuum* **12**, 203 (1962).
28. Gai, L. P., and Kourtakis, K., *Science* **67**, 661 (1995).
29. Taufiq-Yap, Y. H., Sakakini, B. H., and Waugh, K. C., *Catal. Lett.* **46**, 273–277 (1997).
30. To be published.